

See discussions, stats, and author profiles for this publication at: <https://www.researchgate.net/publication/231435934>

# Determination of formal potentials of chemically unstable redox couples by second-harmonic alternating current voltammetry and cyclic voltammetry. Application to the oxidation of t...

ARTICLE *in* JOURNAL OF THE AMERICAN CHEMICAL SOCIETY · AUGUST 1993

Impact Factor: 12.11 · DOI: 10.1021/ja00070a026

---

CITATIONS

34

---

READS

15

## 4 AUTHORS, INCLUDING:



Claude Andrieux

Paris Diderot University

126 PUBLICATIONS 5,489 CITATIONS

SEE PROFILE



Jean Pinson

Paris Diderot University

162 PUBLICATIONS 7,527 CITATIONS

SEE PROFILE

# Determination of Formal Potentials of Chemically Unstable Redox Couples by Second-Harmonic Alternating Current Voltammetry and Cyclic Voltammetry. Application to the Oxidation of Thiophenoxide Ions

Claude P. Andrieux, Philippe Hapiot, Jean Pinson, and Jean-Michel Savéant\*

Contribution from the Laboratoire d'Electrochimie Moléculaire de l'Université de Paris 7, Unité Associée au CNRS No. 438, 2 place Jussieu, 75251 Paris Cedex 05, France

Received March 31, 1993

**Abstract:** In the oxidation of thiophenoxide and para-substituted thiophenoxide ions, the use of second-harmonic ac voltammetry at 25 Hz does not convert reactions that appear chemically irreversible in cyclic voltammetry into reversible systems as implied in previous publications. The reasons for these misinterpretations are unraveled. In spite of a fast dimerization reaction, with a rate constant ranging from  $2 \times 10^8$  to  $2 \times 10^{10} \text{ M}^{-1} \text{ s}^{-1}$ , the use of cyclic voltammetry at micro- and ultramicroelectrodes in appropriate ranges of concentration and scan rate allows the determination of the formal potentials of the  $\text{ArS}^{\bullet}/\text{ArS}^-$  couple with a reasonable accuracy (from 5 to 30 mV). They exhibit a linear correlation with the  $\sigma$  Hammett coefficient with a slope of 0.45 V/unit (the standard potential for the  $\text{PhS}^{\bullet}/\text{PhS}^-$  couple is 0.1 V vs SCE) in acetonitrile.

Reduction and oxidation standard potentials of carbon- or heteroatom-centered radicals are key quantities in the establishment of thermodynamic relationships between radical and ionic chemistries such as those that may be used to derive heterolytic from homolytic bond dissociation energies or vice versa.<sup>1</sup> There are two main avenues of access to these parameters. One is to observe the reduction or oxidation of the radical that may be generated as a transient species by photochemical<sup>2</sup> or direct<sup>3</sup> and indirect<sup>4</sup> electrochemical means. The other starts with the anion, or cation, corresponding to the reduction or oxidation of the radical and uses electrochemical techniques such as cyclic voltammetry to measure a characteristic oxidation, or reduction, potential such as the peak potential in cyclic voltammetry.

The difficulty encountered in relating such potentials to the standard potentials of interest resides in the strong chemical instability of the radical thus generated. For example, in a number of cases, it undergoes rapid coupling with another radical yielding the dimer. If this is the case and if the initial electron-transfer step is fast, the peak potential ( $E_p$ ) and the standard potential ( $E^0$ ) are related by the following equation (for an oxidation reaction)<sup>5</sup> as long as the cyclic voltammetric wave remains

irreversible in the investigated range of scan rates ( $v$ ).<sup>5</sup>

$$E_p = 0.902 \frac{RT}{F} + E^0 - \frac{RT}{3F} \ln \left( \frac{kC^0}{v} \frac{2RT}{3F} \right) \quad (1)$$

( $k$  is the dimerization rate constant and  $C^0$  the bulk concentration of the starting material.) Under such conditions, the standard potential and the rate constant of the follow-up reaction cannot be extracted separately from the experimental data.

The peak potential provides a measure of the standard potential when the scan rate is high enough and/or the concentration  $C^0$  low enough for the cyclic voltammetric wave to be reversible. Then, the standard potential may be obtained as the midpoint between the anodic and cathodic peak potentials.

Second-harmonic alternating current voltammetry<sup>6</sup> (SHACV) has been repeatedly advocated,<sup>1b-d,j,7</sup> including in recent times,<sup>7</sup> as a method of choice to render electrochemical processes where an electron-transfer step is followed by a fast chemically reversible homogeneous chemical step. Several examples have been reported where the same system appears chemically irreversible in cyclic voltammetry and chemically reversible in SHACV even at very low frequencies (25 Hz).<sup>1j,7</sup> These observations are puzzling since the parameter that governs the passage from chemical irreversibility to reversibility is (in the case of a follow-up dimerization)<sup>5,6c</sup>

$$\lambda_{CV} = \frac{RT}{F} \frac{kC^0}{v} \quad \lambda_{SHACV} = \frac{kC^0}{v}$$

for cyclic voltammetry and SHACV, respectively. Therefore, nearly the same degree of reversibility should be obtained at 25 Hz in SHACV and at 0.6 V s<sup>-1</sup> in cyclic voltammetry.

(6) (a) The method consists of applying to the electrode a small amplitude sinusoidal potential on top of a dc potential and detecting the amplitude and phase of the second-harmonic current response. The result of the detection is usually displayed as the variation of the second-harmonic current amplitude with the dc potential in phase and out of phase with the input sinusoidal potential, respectively.<sup>6b</sup> (b) Smith, D. E. AC Polarography and Related Techniques: Theory and Practice. *Electroanalytical Chemistry*; Bard, A. J., Ed.; Dekker: New York, 1966; Vol. 1, pp 1–156. (c) McCord, T. G.; Smith, D. E. *Anal. Chem.* 1968, 40, 1959.

(7) (a) Arnett, E. M.; Amarnath, K.; Harvey, N. O.; Cheng, J.-P.; Venimadhavan, S. *J. Am. Chem. Soc.* 1990, 112, 7346. (b) Venimadhavan, S.; Amarnath, K.; Harvey, N. O.; Cheng, J.-P.; Arnett, E. M. *J. Am. Chem. Soc.* 1992, 114, 221. (c) Arnett, E. M.; Venimadhavan, S.; Amarnath, K. *J. Am. Chem. Soc.* 1992, 114, 5598. (d) Arnett, E. M.; Flowers, R. *Chem. Soc. Rev.* 1993, 9.

(1) (a) See for example, refs 1b–j. (b) Breslow, R.; Goodin, R. *J. Am. Chem. Soc.* 1976, 98, 6076. (c) Breslow, R.; Grant, J. L. *J. Am. Chem. Soc.* 1977, 99, 7745. (d) Jaun, B.; Schwarz, J.; Breslow, R. *J. Am. Chem. Soc.* 1980, 102, 5741. (e) Bordwell, F. G.; Cheng, J.-P.; Harrelson, J. A., Jr. *J. Am. Chem. Soc.* 1988, 110, 1229. (f) Bordwell, F. G.; Bausch, M. J. *J. Am. Chem. Soc.* 1986, 108, 1979. (g) Nicholas, A.; Mide, P.; Arnold, D. R. *Can. J. Chem.* 1982, 20, 2165. (h) Friedrich, L. E. *J. Org. Chem.* 1983, 48, 3851. (i) Arnett, E. M.; Harvey, N. G.; Amarnath, K.; Cheng, J. P. *J. Am. Chem. Soc.* 1989, 111, 4143. (j) Arnett, E. M.; Amarnath, K.; Harvey, N. O.; Cheng, J.-P. *J. Am. Chem. Soc.* 1990, 112, 344.

(2) (a) Wayner, D. D. M.; Griller, D. *J. Am. Chem. Soc.* 1985, 107, 7764. (b) Sim, B. A.; Griller, D.; Wayner, D. D. M. *J. Am. Chem. Soc.* 1989, 111, 754. (c) Griller, D.; Martino Simoes, J. A.; Mulder, P.; Sim, B. A.; Wayner, D. D. M. *J. Am. Chem. Soc.* 1989, 111, 7832. (d) Sim, B. A.; Milne, P. H.; Griller, D.; Wayner, D. D. M. *J. Am. Chem. Soc.* 1990, 112, 6635.

(3) Andrieux, C. P.; Gallardo, I.; Savéant, J.-M. *J. Am. Chem. Soc.* 1989, 111, 1620.

(4) Occhialini, D.; Kristensen, J.-S.; Daasberg, K.; Lund, H. *Acta Chem. Scand.* 1992, 46, 474.

(5) (a) Savéant, J.-M.; Vianello, E. C. R. *Heb. Seances Acad. Sci.* 1963, 256, 2597. (b) Nadjio, L.; Savéant, J.-M. *J. Electroanal. Chem. Interfacial Electrochem.* 1973, 48, 113. (c) Andrieux, C. P.; Savéant, J.-M. *Electrochemical Reactions. Investigation of Rates and Mechanisms of Reactions, Techniques of Chemistry*; Bernasconi, C. F., Ed.; Wiley: New York, 1986; Vol. VI/4E, Part 2, pp 305–390.

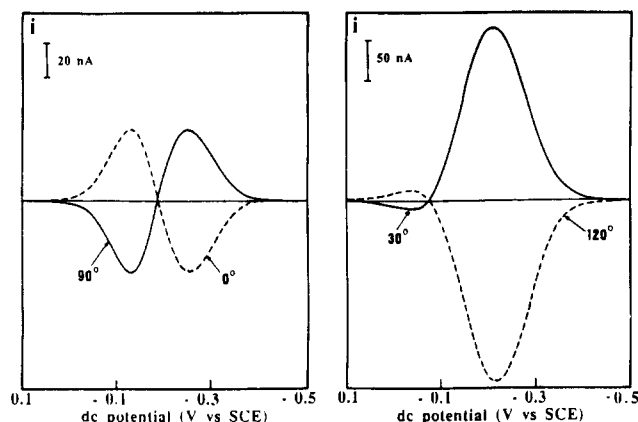


**Figure 1.** Examples of SHACV signals (i) obtained for the reduction of the tetramethylammonium salt of 4-methoxythiophenoxide (5 mM) in a 95:5 sulfolane-3-methylsulfolane mixture containing 0.1 M  $n\text{-Bu}_4\text{NBF}_4$  as the supporting electrolyte at a 1-mm platinum disk electrode: frequency, 25 Hz; amplitude of the sinusoidal potential, 60 mV; temperature, 20 °C. The number on each curve is the nominal value (deg) of the phase angle at which the second-harmonic current response was detected.

One purpose of the following discussion was to unravel the causes of this apparent contradiction. The anodic oxidation of thiophenoxide ions will be taken as illustrative example since it gives rise to a fast but clean coupling of the corresponding radicals yielding the disulfide dimer.<sup>8</sup> The other was to critically establish by means of available electrochemical techniques the values of the formal potential of diversely substituted thiophenoxide ions so as to obtain a Hammett plot that may then be used in various thermodynamic and kinetic applications. Among these, the comprehension of reactivity and selectivity vs structure relationships in  $\text{S}_{\text{RN}}1$  substitutions<sup>9</sup> is particularly relevant to the present study since thiophenoxide ions are among the most commonly used nucleophiles in these reactions.

## Results and Discussion

**Application of Second-Harmonic Alternating Current Voltammetry.** The SHACV responses for the oxidation of the tetramethyl ammonium salt of 4-methoxythiophenoxide in a sulfolane-3-methylsulfolane (5%) mixture were investigated as a function of the phase angle using the same apparatus and experimental conditions as in ref 7b. Typical examples of the signals thus obtained are shown in Figure 1. As seen in more detail later on, the cyclic voltammetric responses under the same conditions are chemically irreversible from 0.1 to 20 000  $\text{V s}^{-1}$ . Among the various traces represented in Figure 1, we draw attention on those corresponding to nominal values of the phase angle equal to 90 and 0°. Both traces exhibit two equal lobes and are symmetrical to one other. These traces are similar, even more symmetrical around the intersection with the dc potential axis, to those reported in ref 7b for a phase angle of 80° for the same alternating potential amplitude. Looking only at these two values of the phase angle, one would have the impression that the electrochemical reaction

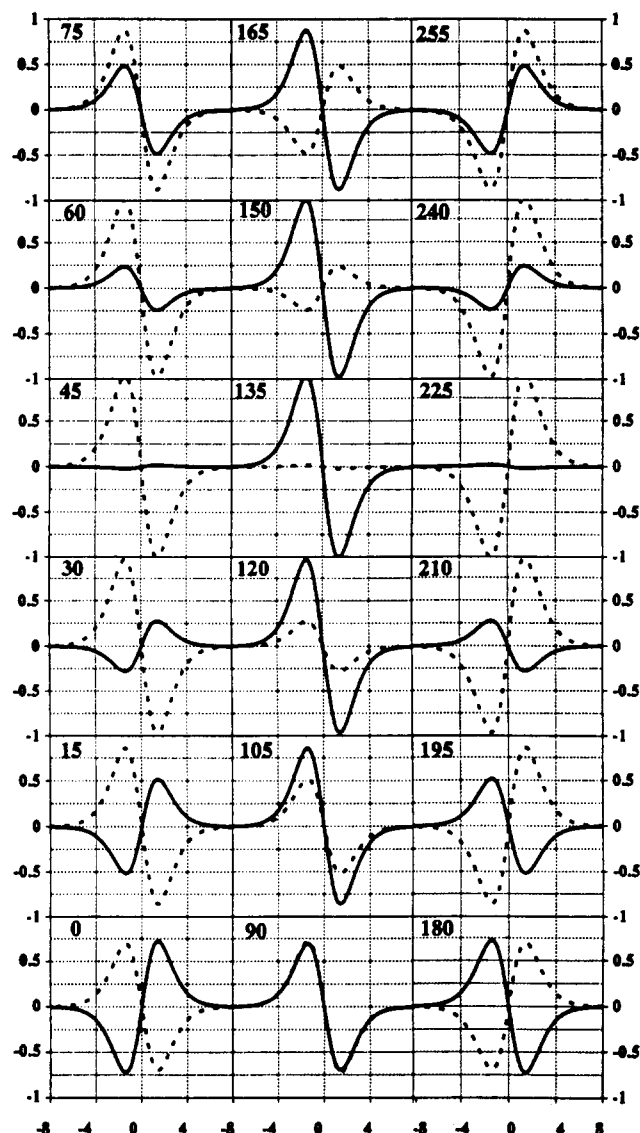


**Figure 2.** Theoretically expected second-harmonic responses for a chemically reversible and electrochemically fast system as a function of the phase angle. The full line represents the response for the indicated phase angle and the dashed line the response for the same phase angle plus 90°. The horizontal axis is  $(RT/F)(E^\circ - E)$  where  $E$  is the dc potential and  $E^\circ$  the standard potential of the chemically reversible couple. The vertical axis is normalized toward the maximal value of the current. The amplitude of the alternating potential is  $\Delta E = RT/F$ , i.e., 25 mV at 25 °C. The full lines correspond to the phase angle (deg) indicated on each diagram. The dashed lines correspond to the same phase angle plus 90°.

has reached chemical reversibility since the two traces then show the typical features of a reversible system.<sup>6b</sup> However, the two lobes cease to be equal upon changing the phase angle value (although the traces obtained at phase angles nominally differing by 90° remain symmetrical around the dc potential axis).

To clear up the situation, it is necessary to consider in more detail the response expected for a chemically reversible system. The traces to be obtained at a given phase angle and at the same phase angle plus 90° are shown in Figure 2, for a series of phase angles with an increment of 15°. The variation of the peak height of the first lobe met upon going from negative to positive potential with the phase angle is depicted in Figure 3 (full lines). The calculations leading to the curves in Figures 2 and 3 are described in the Appendix. We see (Figure 2) that main characteristics of a chemically reversible system are that the positive and negative lobes are symmetrical around the point of intersection with the dc potential axis and that this is located at the standard potential whatever the phase angle. The responses obtained at a given

(8) (a) The oxidation of phenoxide ions gives rise to other types of dimers through carbon oxygen and carbon/carbon coupling as well as to polymers. Reliable values of the standard potential have been obtained by means of cyclic voltammetry when steric hindrance slows down these coupling reactions (see ref 8b and references cited therein). (b) Hapiot, P.; Pinson, J.; Yousfi, N. *New J. Chem.* 1992, 16, 877.

(9) (a) Bunnett, J. F. *Acc. Chem. Res.* 1978, 11, 413. (b) Rossi, R. A.; Rossi, R. H. *Aromatic Substitution by the  $\text{S}_{\text{RN}}1$  Mechanism*. ACS Monograph 178; The American Chemistry Society: Washington, DC, 1983. (c) Savéant, J.-M. *Acc. Chem. Res.* 1980, 13, 323. (d) Savéant, J.-M. *Adv. Phys. Org. Chem.* 1990, 26, 1. (e) Pinson, J.; Savéant, J.-M. *Electrochemical Induction of  $\text{S}_{\text{RN}}1$  Nucleophilic Substitution*. *Electroorganic Synthesis. Festschrift for Manuel M. Baizer*; Little, R. D., Weinberg, N. L., Eds.; Dekker: New York, 1991; pp 29-44.

(10) Above these scan rates, the distortion of the wave is such that it ceases to provide any meaningful information.

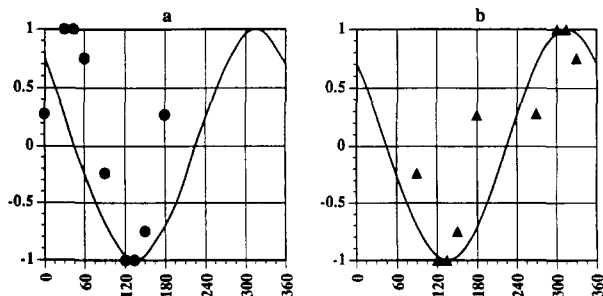


**Figure 3.** Normalized peak height of the first lobe (from negative to positive potentials) of the second-current response for a chemically reversible and electrochemically fast system as a function of the phase angle  $\Delta E = RT/F$ . The full line represents the theoretical expectations in a and b. The points represent the experimental data obtained with the oxidation of ferrocene (see the caption of Figure 4 for experimental conditions) uncorrected (●) and corrected (▲) as explained in the text.

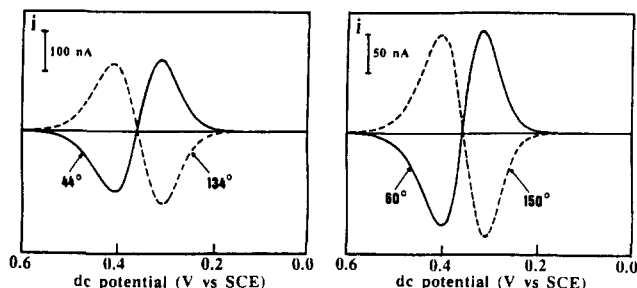


**Figure 4.** SHACV signals (i) obtained for the reduction of ferrocene (2 mM) in a 95:5 sulfolane–3-methylsulfolane mixture containing 0.1 M  $n\text{-Bu}_4\text{NBF}_4$  as supporting electrolyte at a 1-mm gold disk electrode: frequency, 25 Hz; amplitude of the sinusoidal potential, 25 mV; temperature, 20 °C. The number on each curve is the nominal value (deg) of the phase angle at which the second-harmonic current response was detected.

phase angle and at the same phase angle plus 90° are not always symmetrical around the horizontal axis. This happens only when the phase angle is 0 or 180°.

Figure 4 shows some of the responses that we have obtained with a chemically reversible system, namely ferrocene in the 95:5 sulfolane–3-methylsulfolane mixture, using the same instrument as in Figure 1 and in ref 7b. It appears that, at any accessible nominal value of the phase angle, the response and the response at the same value plus 90° are symmetrical around the dc potential axis. This does not match the theoretical expectations as discussed above. It appears, as can be seen also from other results displayed in Figure 3, that the nominal values of the phase angle comprised between 90 and 180° (including 90) are approximately correct whereas the values comprised between 0 and 90° (including 0) are not. 90° should be subtracted, or equivalently, 270° should be added to the latter values to obtain meaningful results. This artifact in the instrument is the reason that nominal values nominally differing by 90° appear to give symmetrical responses. At each nominal value, however, the symmetry of the positive and negative lobes and the independence of the intersection toward the phase angle do appear, as predicted for chemically reversible systems. We also note in Figure 3 that the accuracy in the values of the phase angle, even corrected as described above, is rather poor, as expected for the detection (or extraction) from a global ac response of second-harmonic signals that are necessarily small in front of the first-harmonic responses. Thus with this type of instrumentation, the demonstration of chemical reversibility relies more on the symmetry of the positive and negative lobes and the constancy of the intersection point upon varying the phase angle in the accessible range of values rather than on a quantitative reproduction of all the theoretical expectations such as, for example, the variation of the lobe heights with the phase angle.

We may now come back to the responses observed with the oxidation of 4-methoxythiophenoxide ions (Figure 1). The observation that in each of the two cases, the responses obtained with phase angles differing nominally by 90° are symmetrical around the intersection point is not an indication that the electrochemical reaction is chemically reversible. As shown above, the actual difference between the phase angles is 180°. Then not only chemically reversible but also chemically irreversible systems give rise to symmetrical traces as shown below. The equality of the two lobes is observed for one nominal value of the phase angle of 90° (and 270°) but not for other values of the phase angle as exemplified in Figure 1 for the nominal value 120° (and 300°). If the reaction is chemically reversible, the two lobes should be equal whatever the phase angle. Also, the intersection with the dc potential axis varies considerably with the phase angle: −0.18 V vs SCE for 90° (and 270°), −0.08 V vs SCE for 120° (and 300°). We may thus conclude that the reaction is not in fact chemically reversible. The experimental data actually conform to compete chemical irreversibility. Figure 5 shows the second-harmonic responses theoretically expected for a rapid electron-transfer step followed by a fast and irreversible dimerization of the radicals formed in the first step (see the Appendix for the computation method we used). We have checked that slow charge transfer and uncompensated  $iR$  drop may affect the exact shape of the lobes, tending to draw them out along the dc potential axis, but not their general aspect, particularly their symmetry or lack of symmetry.

It can be seen that one phase angle (and the same plus 180°) exists for which the two lobes are symmetrical around the intersection point but that, unlike the reversible case, the symmetry disappears as soon as the phase angle deviates from this value. The experimental data shown in Figure 1, and those reported in ref 7b, are thus perfectly consistent with a totally irreversible reaction involving the follow-up dimerization of the radicals generated in the initial electron-transfer step and not with a chemically reversible reaction. The experimental value of the phase angle at which symmetry is observed does not accord exactly with the theoretical predictions. This is not too surprising since the experimental values of the phase angle are rather imprecise as discussed above when examining the responses obtained with the reversible ferrocene/ferrocenium couple.

The potential,  $E_i$ , corresponding to the intersection with the dc potential axis at the phase angle where the two lobes are symmetrical is related to the standard potential of the anion/radical couple,  $E^0$ , by the following equation (see the Appendix)

$$E_i = E^0 - 0.70 \frac{RT}{F} - \frac{RT}{3F} \ln \left( \frac{2kC^0}{3\nu} \right)$$

( $\nu$  = frequency,  $k$  = dimerization rate constant, and  $C^0$  = bulk concentration of the substrate.) Thus for typical values as  $\nu$  = 25 Hz,  $k$  =  $10^{10} \text{ M}^{-1} \text{ s}^{-1}$  (the dimerization rate constants of the thiophenoxide radical are not far from the diffusion limit as seen below), and  $C^0$  = 2 mM, the measured potential  $E_i$  would be 115 mV to the negative of the actual standard potential. This (2.7 kcal/mol) may appear or not as an acceptable error depending upon the application. The important point we wish to make here is that the potential thus determined is not the reversible formal potential required in thermochemical applications.

**Determination of the  $\text{ArS}^{\bullet}/\text{ArS}^-$  Formal Potentials by Cyclic Voltammetry.** We investigated the oxidation of thiophenoxide ions and of 4-methoxy, 4-methyl-, 4-chloro- and 4-nitrophenoxide ions in acetonitrile. They all give rise to chemically irreversible cyclic voltammetric waves between 0.1 and 100  $\text{V s}^{-1}$  of the type shown in Figure 6 for the case of 4-methylthiophenoxide. With this compound and 4-methoxythiophenoxide, the anodic peak potential varies linearly with  $\log \nu$  ( $\nu$  = scan rate) with a slope of 20 mV/unit (Figure 6). These observations indicate that within this range of scans the reaction mechanism consists of a rapid

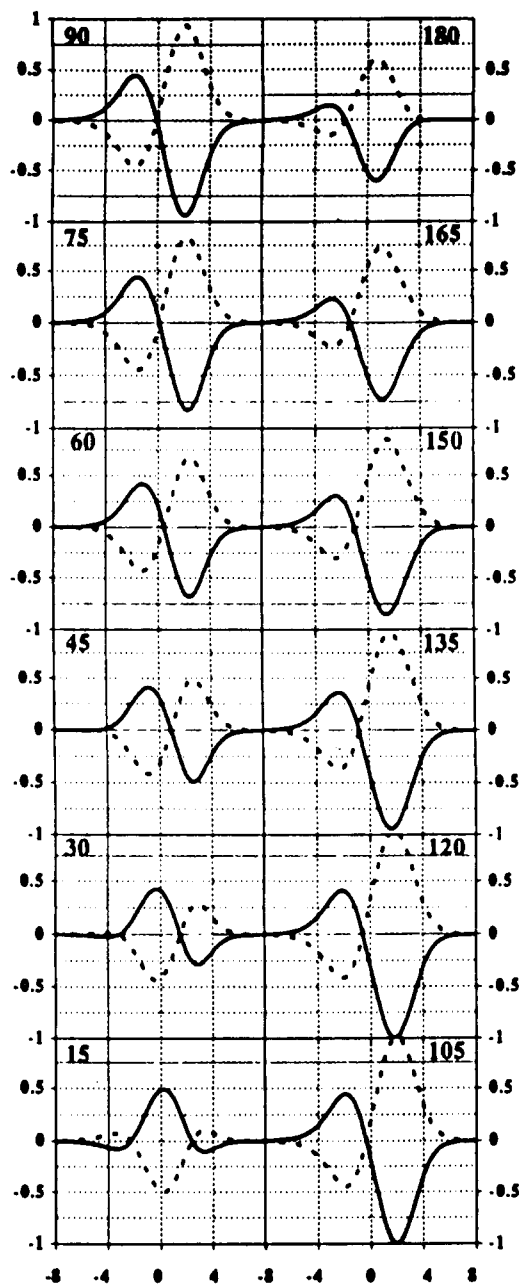
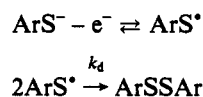


**Figure 5.** Theoretically expected second-harmonic responses for a chemically irreversible system involving a fast electrochemical step followed by a fast and irreversible dimerization. The horizontal axis is  $(RT/F)(E^* - E)$  where  $E$  is the dc potential and  $E^* = E^0 - RT/3F \ln(2kC^0/3\nu)$  ( $E^0$  = standard potential of the initial step,  $k$  = rate constant of dimerization,  $C^0$  = bulk concentration of the substrate, and  $\nu$  = frequency.) The vertical axis is normalized toward the maximal value of the current. The amplitude of the alternating potential is  $\Delta E = 2.4 RT/F$ , i.e., 60 mV at 25 °C. The full lines correspond to the phase angle (deg) indicated on each diagram. The dashed lines correspond to the same phase angle plus 180°.

electron-transfer step followed by a fast and irreversible dimerization reaction:<sup>5</sup>



Using the same low concentration as in the experiments in Figure 6, partial chemical reversibility could be reached at 1000 V s<sup>-1</sup> for both the 4-methoxy and 4-methyl derivatives at a standard 1-mm-diameter electrode (Figure 7). The role of a low substrate

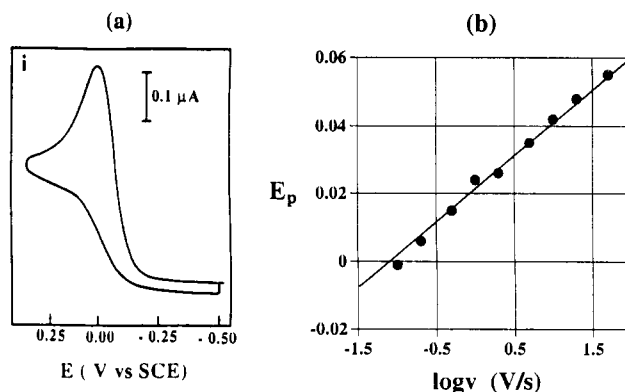


**Figure 6.** Cyclic voltammetry of 4-methylthiophenoxide ions (0.08 mM) in acetonitrile plus 0.1 M Et<sub>4</sub>NBF<sub>4</sub> at a 1-mm-diameter gold disk electrode. (a) Cyclic voltammogram at 0.2 V s<sup>-1</sup>. (b) Variation of the anodic peak potential,  $E_p$  (V vs SCE), with the scan rate ( $\nu$ ) (temperature = 20 °C).

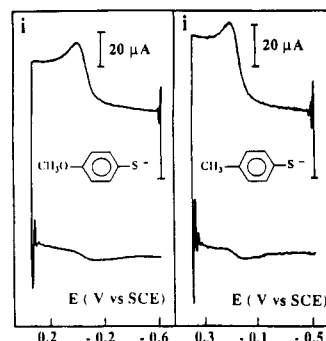


**Figure 7.** Cyclic voltammetry of 4-methoxy and 4-methylthiophenoxide ions (0.08 mM) at 1000 V s<sup>-1</sup> in acetonitrile plus 0.1 M Et<sub>4</sub>NBF<sub>4</sub> at a 1-mm-diameter gold electrode (temperature = 20 °C).

concentration is to decrease the parameter  $\lambda = (kC^0/\nu)(RT/F)$  which governs the competition between diffusion and the second-order follow-up chemical reaction and thus to facilitate the passage to chemical reversibility upon raising the scan rate.<sup>5</sup> The formal potential of the  $\text{ArS}^*/\text{ArS}^-$  couple could be then determined as the midpoint between the anodic and cathodic peak potentials. Their values are reported in Figure 9. From these values and those of the peak potentials at low scan rates, the dimerization rate constants of the radicals are found, by application of eq 1, to be  $k_d = 5 \times 10^8$  and  $2 \times 10^8 \text{ M}^{-1} \text{ s}^{-1}$  for the methoxy and methyl derivatives, respectively.

No such reversibility was found with the other three derivatives (H, Cl, and NO<sub>2</sub>). The peak potentials of the irreversible wave observed at 0.1 V s<sup>-1</sup> are 0.050, 0.100, 0.410 for the H, Cl, and NO<sub>2</sub> derivatives at concentrations of 0.05, 0.08, and 0.05 mM, respectively. Neither did the waves obtained with these compound at a 10-μm-diameter electrode with a 0.2 mM concentration show any sign of reversibility up to 20 000 V s<sup>-1</sup>. It follows that for these three compounds  $k_d \geq 2 \times 10^9 \text{ M}^{-1} \text{ s}^{-1}$ ,<sup>5</sup> in keeping with the value found for PhS<sup>•</sup> in water,  $k_d = 9.6 \times 10^9 \text{ M}^{-1} \text{ s}^{-1}$ .<sup>11</sup> On the other hand, the dimerization rate constant is smaller than the diffusion limit; thus for all three compounds (in M<sup>-1</sup> s<sup>-1</sup>)

$$2 \times 10^9 \leq k_d \leq 2 \times 10^{10}$$

The variation of the peak potentials of each of these three derivatives does not conform to the 20 mV/unit linear variation with the logarithm of the scan rate, between 0.1 and 100 V s<sup>-1</sup>, as was the case for the methoxy and methyl derivatives. Instead a continuous variation of the type shown in Figure 8 for the case of 4-chlorothiophenoxide ions is observed. This behavior indicates a mixed kinetic control of the reaction by the initial electron-

(11) Tripathi, G. N. R.; Sun, Q.; Armstrong, D. A.; Chipman, D. M.; Schuler, R. H. *J. Phys. Chem.* **1992**, *96*, 5344.

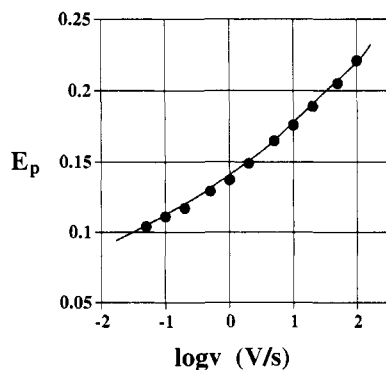


**Figure 8.** Cyclic voltammetry of 4-chlorothiophenoxide ions (0.08 mM) in acetonitrile plus 0.2 M Et<sub>4</sub>NBF<sub>4</sub> at a 1-mm-diameter gold disk electrode. Anodic peak potential,  $E_p$  (in V vs SCE), as a function of the scan rate (temperature = 20 °C). The full line is theoretically predicted variation for  $k_s^2/Dk_d^{1/3} = 0.7 \text{ mol}^{1/3} \text{ s}^{-2/3}$ .

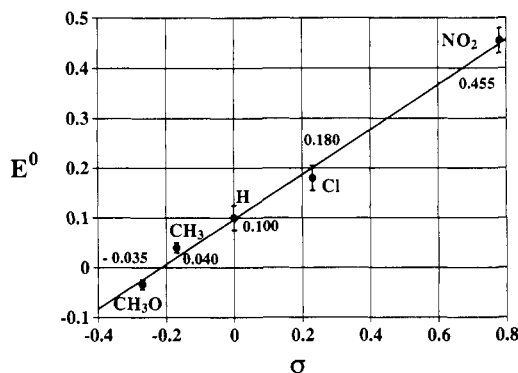


**Figure 9.** Formal potential for the oxidation of thiophenoxide and para-substituted thiophenoxide ions as a function of the Hammett  $\sigma$  coefficient.

transfer step and the follow-up dimerization step.<sup>5</sup> The competition between the two steps is governed by the parameter<sup>5b</sup>

$$p = \left( \frac{RT}{Fv} \right)^{2/3} k_s^2 k_d^{-1/3} C_0^{-1/3} D^{-1}$$

(assuming that the transfer coefficient is 0.5) where  $D$  is the diffusion coefficient of the substrate and  $k_s$  is the standard rate constant of electron transfer uncorrected from double-layer effects. Fitting of the experimental points by the theoretically predicted variations leads to the following values of  $k_s^2/Dk_d^{1/3}$  (in  $\text{mol}^{1/3} \text{ s}^{-2/3}$ )

H: 1.1      Cl: 0.7      NO<sub>2</sub>: 0.8

Assignment of a value to  $k_d$ , comprised between  $2 \times 10^9$  and  $2 \times 10^{10} \text{ M}^{-1} \text{ s}^{-1}$ , allows the determination of  $E^0$  by adjustment of the theoretical and experimental  $E_p - \log v$  curves. The values of  $E^0$  reported in Figure 9 correspond to the middle of the interval of possible  $k_d$  values, i.e.,  $6.3 \times 10^9 \text{ M}^{-1} \text{ s}^{-1}$ . The uncertainty on  $k_d$  leads to a  $\pm 25 \text{ mV}$  systematic error on  $E^0$ . Adding to this the  $\pm 5\text{-mV}$  experimental error leads to an uncertainty of  $\pm 30 \text{ mV}$ , i.e., of  $\pm 0.7 \text{ kcal/mol}$  for thermochemical applications. The uncertainty on  $E^0$  is less for the methoxy and methyl derivative,  $\pm 5 \text{ mV}$ , i.e.,  $0.1 \text{ kcal/mol}$ .

## Conclusions

Second-harmonic ac techniques at 25 Hz do not convert reactions that appear irreversible in slow-scan cyclic voltammetry into chemically reversible systems. Previous implications<sup>11,7</sup> of the contrary derived from instrumentation and interpretation artifacts. Cyclic voltammetry in appropriately selected ranges of substrate concentration and scan rate allowed the determination of the formal potential of a series of ArS<sup>•</sup>/ArS<sup>-</sup> couples where the rate constant of the follow-up dimerization ranges from  $2 \times$

$10^8$  to  $2 \times 10^{10} \text{ M}^{-1} \text{ s}^{-1}$ , with a precision that appear reasonable for future thermochemical applications. As seen in Figure 9, the formal potentials thus obtained exhibit a linear correlation with the Hammett  $\sigma$  coefficient with a slope of 0.45 V/unit.

## Experimental Section

**Chemicals.** Spectrograde acetonitrile from Merck (uvasol grade) was used as received. The sulfolane-3-methylsulfolane mixture was prepared as described in ref 1j. The tetraethyl- and tetra-*n*-butylammonium tetrafluoroborates used as supporting electrolyte were from Fluka (puriss grade) and were used as received.

The thiophenoxide salts were prepared in the electrochemical cell under argon by neutralization of the corresponding thiophenols (from Aldrich) by a methanol solution of tetramethylammonium hydroxide (5H<sub>2</sub>O, concentration 2.2 M).

**Instrumentation.** The second-harmonic ac experiments were carried out with a BAS 100A (BAS, West Lafayette, IN,) as in refs 1j and 7.

For cyclic voltammetry below  $1000 \text{ V s}^{-1}$ , we used a home-built potentiostat equipped with positive feedback  $iR$  drop compensation,<sup>12a</sup> a PAR model 175 Universal Programmer function generator, and a 310 Nicolet digital oscilloscope. At these scan rates, the working electrode was a 1-mm-diameter gold or platinum electrode polished with a 1- $\mu\text{m}$  diamond paste and rinsed ultrasonically in ethanol before use.

In the high scan rate experiments, we used a Hewlett Packard 3314A function generator, a 450 Nicolet digital oscilloscope (5 ns per point minimum acquisition time), and another home-built potentiostat.<sup>12b</sup> The ultramicroelectrode was a 10- $\mu\text{m}$ -diameter gold disk polished before use as described above.

The electrochemical cell was thermostated at  $20 \pm 0.1 \text{ }^\circ\text{C}$ . The reference electrode was an aqueous SCE separated from the test solution by a salt bridge containing the supporting electrolyte. Its potential was checked against the ferrocene/ferrocenium couple before and after each experiment.

## Appendix

The theoretically predicted SHACV responses were computed as follows. The variation of the dc potential induces a steady-state variation of the dc current which derives from the existence of a diffusion-convection layer established by means of natural convection, the thickness of which is of the order of  $2 \times 10^{-2} \text{ cm}$ .<sup>13</sup> The concentration profile of the substrate both in the chemically reversible and irreversible case is assumed to be linear and is defined by  $C^0$  (the bulk concentration) at the boundary of the diffusion convection layer and a value that depends on the dc potential at the electrode surface. The addition of an alternating potential to the dc potential triggers a periodical variation of the substrate concentration around the dc profile in the vicinity of the electrode surface. The thickness of this second diffusion layer is of the order of  $(\pi D/\nu)^{1/2}$ , where  $D$  is the diffusion coefficient of the substrate and  $\nu$  the frequency, i.e.,  $10^{-3} \text{ cm}$  for  $\nu = 25 \text{ Hz}$ , 20 times thinner than the diffusion-convection layer. As the ratio of the ac to the dc reaction layer between the thicknesses of these two reaction layers decreases, the alternating current response becomes independent of the ratio. What is intended by the alternating current response is the response obtained after a sufficient number of cycles for the signal to reach a steady state. The latter was reached with a good precision after 15–30 cycles.

The substrate concentration,  $C$ , obeys the second Fick's law:

$$\frac{\partial C}{\partial t} = D \frac{\partial^2 C}{\partial x^2}$$

( $t$  = time and  $x$  = the distance from the electrode surface.)

(12) (a) Garreau, D.; Savéant, J.-M. *J. Electroanal. Chem. Interfacial Electrochem.* **1972**, 35, 309. (b) Garreau, D.; Hapiot, P.; Savéant, J.-M. *J. Electroanal. Chem. Interfacial Electrochem.* **1989**, 272, 1.

(13) Andrieux, C. P.; Hapiot, P.; Savéant, J.-M. *J. Electroanal. Chem. Interfacial Electrochem.* **1993**, 349, 299.

Normalizing the concentration, time, and distance as follows

$$a = \frac{C}{C^0} \quad \tau = \nu t \quad y = x(\nu/D)^{1/2}$$

the diffusion equation becomes

$$\frac{\partial a}{\partial \tau} = \frac{\partial^2 a}{\partial y^2}$$

This was numerically solved by an explicit finite difference method<sup>14</sup> with an elementary time interval  $\Delta\tau = 0.01$  and a space interval  $\Delta y = 0.15$ .

The boundary condition for  $y \rightarrow \infty$  is  $a = 1$ .

At the electrode surface, in the reversible case

$$a = \frac{1}{1 + \exp\left[-\frac{F}{RT}(E - E^0)\right]}$$

where  $E^0$  is the standard potential and  $E$  the electrode potential

$$E = E_{dc} + \Delta E \sin 2\pi\nu t$$

( $E_{dc}$  is the dc potential.) Introducing

$$\xi = (F/RT)(E^0 - E) \text{ and } \Delta\xi = (F/RT) \Delta E,$$

$$\xi = \xi_{dc} + \Delta\xi \sin 2\pi\tau$$

and, at the electrode surface,

$$a = \frac{1}{1 + e^\xi}$$

The calculations of the dimensionless current function

$$\Psi = \left(\frac{da}{dy}\right)_{y=0} = \frac{i}{FSC^0D^{1/2}\nu^{1/2}}$$

( $S$  = electrode surface area) were carried out from  $\xi = -8$  to 8 with a 0.5 increment with a number of  $y$  elementary intervals of 15–30.

Once the steady-state responses have been thus obtained, a Fourier series development

$$\Psi = \Psi_{dc} + \sum_{n=1}^{\infty} A_n \cos 2\pi n\tau + B_n \sin 2\pi n\tau$$

is carried out for each  $\xi$  value by means of

$$A_n = 2 \int_0^1 \Psi(\tau) \cos 2\pi n\tau \, d\tau$$

$$B_n = 2 \int_0^1 \Psi(\tau) \sin 2\pi n\tau \, d\tau$$

and the dimensionless second-harmonic response finally obtained from its amplitude  $(A_2^2 + B_2^2)^{1/2}$  and phase,  $\arctan(A_2/B_2)$ .

The irreversible case was treated in a similar manner, replacing the electrode surface boundary condition by

$$\Psi^{2/3} \exp(-\xi^*) = 1 - \Psi$$

where

$$\xi^* = \xi - \frac{1}{3} \ln(2\lambda/3) \quad \lambda = kC^0/\nu$$

a condition which characterizes a fast and irreversible dimerization following a fast electron-transfer step.<sup>5</sup>

**Acknowledgment.** We gratefully thank Dr. Antoine Demortier (Laboratoire de Chimie-Physique de L'Ecole des Hautes Etudes Industrielles, Lille, France) for the permission to use his BAS 100 machine and for very helpful advice concerning the operating procedures.